

RESEARCH ARTICLE

Bringing up to date the toolkit for the catabolism of aromatic compounds in fungi: The unexpected 1,2,3,5-tetrahydroxybenzene central pathway

Tiago M. Martins  | Artur Bento  | Celso Martins  | Ana S. Tomé  |
Carlos J. S. Moreira  | Cristina Silva Pereira 

Instituto de Tecnologia Química e Biológica António Xavier, Universidade Nova de Lisboa (ITQB NOVA), Oeiras, Portugal

Correspondence

Cristina Silva Pereira, Instituto de Tecnologia Química e Biológica António Xavier, Universidade Nova de Lisboa (ITQB NOVA), Av. da República, 2780-157 Oeiras, Portugal.
Email: spereira@itqb.unl.pt

Present address

Celso Martins, Center for Integrative Genomics, Faculty of Biology and Medicine, University of Lausanne, Lausanne, Switzerland

Funding information

National Funds from Portugal2020, Grant/Award Number: 13/SI/2020-072630; Fundação para a Ciência e a Tecnologia; MOSTMICRO-ITQB R&D Unit, Grant/Award Number: UIDP/04612/2020 and UIDB/04612/2020; LS4FUTURE Associated Laboratory, Grant/Award Number: LA/P/0087/2020; National Funds under Norma Transitória D.L., Grant/Award Number: 57/2016; Fellowship SFRH/BD/118377/2016

Abstract

Saprophytic fungi are able to catabolize many plant-derived aromatics, including, for example, gallate. The catabolism of gallate in fungi is assumed to depend on the five main central pathways, i.e., of the central intermediates' catechol, protocatechuate, hydroxyquinol, homogentisate and gentisate, but a definitive demonstration is lacking. To shed light on this process, we analysed the transcriptional reprogramming of the growth of *Aspergillus terreus* on gallate compared with acetate as the control condition. Surprisingly, the results revealed that the five main central pathways did not exhibit significant positive regulation. Instead, an in-depth analysis identified four highly expressed and upregulated genes that are part of a conserved gene cluster found in numerous species of fungi, though not in *Aspergilli*. The cluster comprises a monooxygenase gene and a fumarylacetoacetate hydrolase-like gene, which are recognized as key components of catabolic pathways responsible for aromatic compound degradation. The other two genes encode proteins with no reported enzymatic activities. Through functional analyses of gene deletion mutants in *Aspergillus nidulans*, the conserved short protein with no known domains could be linked to the conversion of the novel metabolite 5-hydroxydienelaton, whereas the DUF3500 gene likely encodes a ring-cleavage enzyme for 1,2,3,5-tetrahydroxybenzene. These significant findings establish the existence of a new 1,2,3,5-tetrahydroxybenzene central pathway for the catabolism of gallate and related compounds (e.g. 2,4,6-trihydroxybenzoate) in numerous fungi where this catabolic gene cluster was observed.

INTRODUCTION

Saprophytic fungi play an invaluable role in the turnover of the elements, including those present in highly abundant plant phenolic sources such as lignin and tannins (Mäkelä et al., 2015). Understanding the catabolism of aromatics, for example, gallate, a major intermediate of the metabolism of lignin constituents, esterified polysaccharides and hydrolysable tannins (Mäkelä

et al., 2015), is crucial to decipher the ecological aspects of plant biomass degradation. This process ultimately occurs through the central pathways for the metabolism of key aromatic compounds. Countless peripheral pathways converge towards a small number of central intermediates that undergo ring cleavage in the central pathways. In fungi, there are five main described pathways of the central intermediates: catechol, protocatechuate, hydroxyquinol, homogentisate and gentisate

This is an open access article under the terms of the [Creative Commons Attribution-NonCommercial](https://creativecommons.org/licenses/by-nc/4.0/) License, which permits use, distribution and reproduction in any medium, provided the original work is properly cited and is not used for commercial purposes.

© 2023 The Authors. *Microbial Biotechnology* published by Applied Microbiology International and John Wiley & Sons Ltd.

(Martins et al., 2019), of which the corresponding catabolic genes are known (Gérecová et al., 2015; Holesova et al., 2011; Martins et al., 2015; Mingot et al., 1999; Semana & Powlowski, 2019). The five central pathways are present in the genomes of both Ascomycota and Basidiomycota, sharing high similarity, despite some noteworthy differences (Martins et al., 2019). A catabolic pathway for the central intermediate 3-hydroxyanthranilate was recently discovered in fungi (Martins et al., 2021). The existence of other specific dioxygenases for gallate, hydroquinone, homoprotocatechuate and pyrogallol, as described for bacteria, remains to be verified in fungi, although mostly accepted that these intermediates are channelled into the five main central pathways (Ferrer-Sevillano & Fernandez-Canon, 2007; Gérecová et al., 2015; Patel et al., 1992).

The catabolism of gallate by Ascomycota is assumed to occur through three pathways but none is fully described (schematically represented in Figure 1). First, a path of initial reduction and metabolization to protocatechuate was proposed for *Penicillium simplicissimum* (Patel et al., 1992). Second, it was established

for the yeast *Blastobotrys adenivorans* an initial non-oxidative decarboxylation of gallate to pyrogallol that undergoes intradiol ring cleavage, mediated by a catechol-like dioxygenase, forming 2-hydroxymuconate, which is then channelled to an undisclosed catabolic pathway for 4-oxalocrotonate (Meier et al., 2017; Sietmann et al., 2010). The same pathway was suggested for *Aspergillus* and *Penicillium* species once they also accumulate pyrogallol (Gurujeyalakshmi & Mahadevan, 1987). Finally, direct ring cleavage was proposed for both *A. niger* and *A. flavus*, based on indirect pieces of evidence, including apparent gallate dioxygenase activity (Gurujeyalakshmi & Mahadevan, 1987; Watanabe, 1965). The catabolism of gallate in *A. niger* was further described to be independent of the protocatechuate branch of the 3-oxoadipate pathway (Boschloo et al., 1990). Collectively, data on the catabolism of gallate in fungi suggest that different pathways may be used by closely related species, and possibly exhibit some redundancy.

To better understand the catabolism of gallate, in the present study, we resorted to *A. terreus* and *A. nidulans*

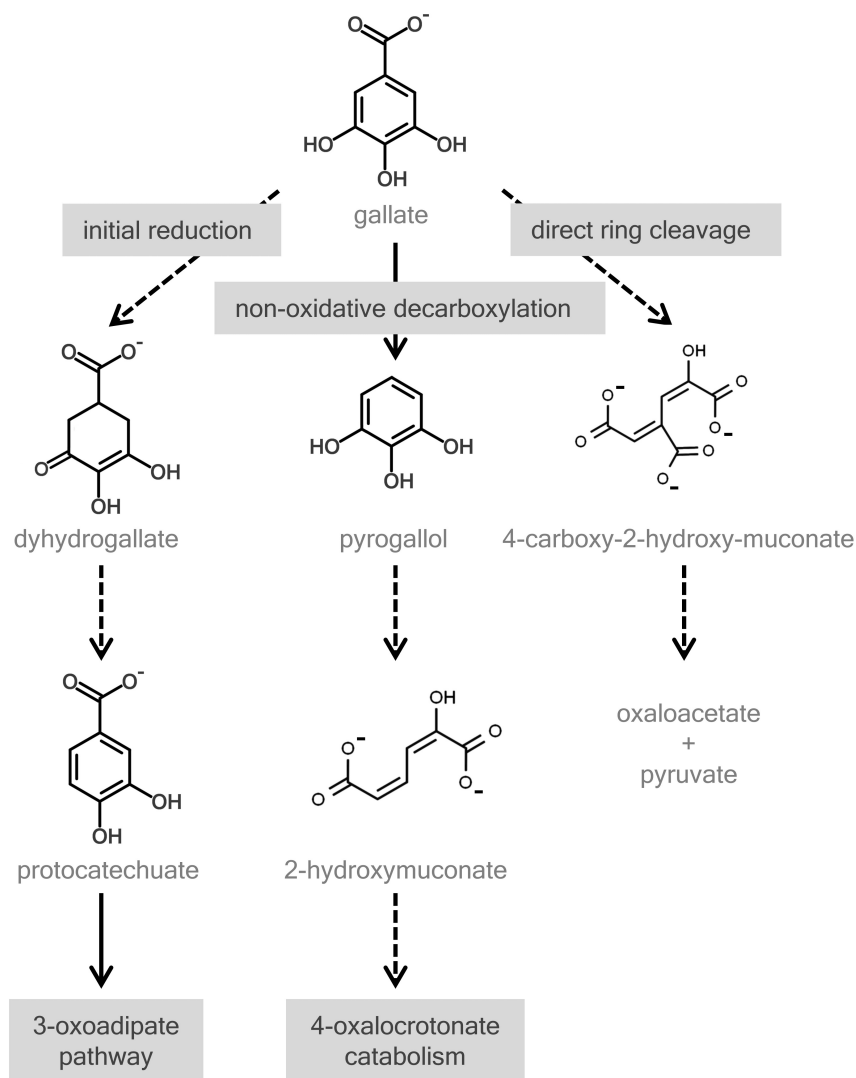


FIGURE 1 The three different proposed gallate catabolic pathways in fungi. Confirmed reactions (solid arrows) and suggested reactions (dashed arrows).

as model fungi. Specifically, the transcriptional response of *A. terreus* growth on gallate was analysed by RNA-seq (acetate was used as a control condition). This was complemented by targeted gene expression analyses in both fungi, functional studies of gene deletion mutants in *A. nidulans*, and analytical chemical identifications of specific intermediates. The data support the elucidation of the catabolism of gallate, and other similar compounds, through a new central pathway with initial hydroxylation (decarboxylating) and formation of the central intermediate 1,2,3,5-tetrahydroxybenzene. Furthermore, genes essential for gallate utilization are organized in a cluster of genes present in several genomes, increasing the relevance of this novel central pathway for fungi in general.

EXPERIMENTAL PROCEDURES

Strains and growth conditions

Aspergillus terreus FGSC A1156 (equivalent NIH2624), *Aspergillus nidulans* FGSC A4, and additional strains (Table S1) asexual spores were harvested and maintained as frozen suspensions at -80°C (Hartmann et al., 2015). Liquid cultures were initiated with 10^6 spores/mL and incubated with orbital agitation (250 rpm) in the dark at 37°C . Batch cultivations were performed in 250-mL Erlenmeyer flasks with a working volume of 50 mL. A low nitrogen minimal medium was used containing *per* litre 3 g NaNO_3 , 0.01 g $\text{ZnSO}_4 \cdot 7\text{H}_2\text{O}$, 0.005 g $\text{CuSO}_4 \cdot 5\text{H}_2\text{O}$, 0.5 g $\text{MgSO}_4 \cdot 7\text{H}_2\text{O}$, 0.01 g $\text{FeSO}_4 \cdot 7\text{H}_2\text{O}$ and 0.5 g KCl. Filter sterilized salts were added to an autoclave sterilized 100-mM potassium phosphate solution. The carbon sources were added either directly to the potassium phosphate solution for sterilization (60-mM sodium acetate—control, pH6.0) or into the mineral media after filter sterilization (e.g. 20 mM gallate, pH4.0). Whenever relevant, the appropriate auxotroph nutrient requirements were added, and agar (10 g L^{-1}) was used to gel the media. Cultures of gene replacement mutants for functional analysis in liquid medium were done in 100-mM potassium phosphate buffer pH5.0 incubated with orbital agitation (250 rpm) in the dark at 30°C using pre-grown mycelium for 24 h in sodium acetate liquid minimal medium. Cultures in solid media (triplicates) were grown for 5 days at 30°C , in \varnothing 50-mm plates.

Chemicals

Gallic acid monohydrate (ACS), 3,4,5-trimethoxyphenol (>98.5%), ascorbic acid (99%) and sodium nitrate (extra pure) were purchased from Acros Organics; 3,4-dihydroxybenzoic acid (97%) from Alfa Aesar;

acetonitrile (>99.9%), ethyl acetate (>99.8%), diethyl ether (>99.5%) and methanol (>99.8%) from Fisher Chemical; sodium hydroxide (>98%) from José Manuel Gomes dos Santos; anhydrous sodium sulphate (99%), boron tribromide solution in anhydrous dichloromethane and anhydrous dichloromethane (99.7%) from Thermo Scientific; agar and resorcinol (99%) from Panreac; all other chemicals of the highest grade from Sigma-Aldrich/Merck.

Synthesis of 1,2,3,5-tetrahydroxybenzene

1,2,3,5-tetrahydroxybenzene was synthesized as previously described (Paizs et al., 2007). A solution of BBr_3 in anhydrous CH_2Cl_2 (1 M, 18.8 mL) was added, with stirring, to a solution of 3,4,5-trimethoxyphenol in anhydrous CH_2Cl_2 (1.88 mmol, 10 mL) at -80°C under nitrogen during 1 h and the reaction was left to warm until room temperature. After overnight, the mixture was cooled to 0°C and distilled water (5 mL) was added. The CH_2Cl_2 was removed under nitrogen flow and the remaining mixture was extracted with ethyl acetate. The organic phase was dried with anhydrous NaSO_4 , filtered and concentrated under nitrogen flow. ^1H NMR (800 MHz, $\text{DMSO}-d_6$): 5.72 (s, 2H); ^{13}C NMR (201 MHz, $\text{DMSO}-d_6$): 94.34; 125.33; 146.77; 149.91.

Metabolite identification and quantification by chromatography

The culture media or the respective ethyl acetate extracts were analysed by liquid chromatography (LC) for the identification and/or quantification of the aromatic compounds and their transformation products using a previously described method (Martins et al., 2014). Two other methods were used depending on the polarity of the compounds of interest. For alternative hydrophobic selectivity compared to the previously mentioned method (with a standard C_{18} column), a Synergi Polar-RP column, $4\ \mu\text{m}$, $150 \times 4.6\ \text{mm}$ (Phenomenex), set at 26°C , was used. For the separation, the eluent (5-mM potassium phosphate pH3.05 with 2% methanol) was used for 6 min under isocratic conditions, followed by a 15-min gradient of increasing percentage of methanol from 2% to 50%, at a flow rate of $0.8\ \text{mL} \cdot \text{min}^{-1}$ (HPLC method A). For increased retention of very hydrophobic compounds, a Synergi Hydro-RP column, $4\ \mu\text{m}$, $250 \times 4.6\ \text{mm}$ (Phenomenex), set at 26°C , was used. The eluent, 20-mM potassium phosphate pH2.9, was used under isocratic conditions at a flow rate of $0.7\ \text{mL} \cdot \text{min}^{-1}$ (HPLC method B).

Samples were analysed by gas chromatography–mass spectrometry (GC–MS) with an Agilent GC (7820A) equipped with a single quadrupole Agilent

(5977B) MS. The ethyl acetate extracts were dried under a soft nitrogen flow, and subsequently derivatized with *N,O*-bis (trimethylsilyl)-trifluoroacetamide containing 1% of trimethylchlorosilane and pyridine (5:1) for 30 min at 90°C. The separation of the analytes was carried out using an HP-5MS column (30 m by 250 µm by 0.24 µm; Agilent) with the following ramp temperature: 80°C, 4°C/min until 290°C for 10 min. Full scan mode with a mass range of *m/z* 40–900, with a source at 230°C and electron impact ionization (EI+, 70 eV), was used for all samples, and acquisition delay was set at 240 s. Technical triplicates were analysed. Data acquisition was accomplished by MSD ChemStation (Agilent) and compounds were identified based on a spectral library (NIST 2017) and references relying on diagnostic ions distinctive of each derivative and its spectrum profile.

The extracts were also analysed by liquid chromatography–mass spectrometry (LC–MS) using a Q Exactive Focus Hybrid Quadrupole-Orbitrap (Thermo Scientific). The separation was achieved in a Waters Acquity UPLC HSS T3 column (2.1 × 150 mm, 1.8 µm particle size), using a gradient of increasing percentage of 0.9% formic acid (FA) in acetonitrile (B) and 0.9% FA in ammonium formate 50 mM (pH 2.9) (C) and decreasing percentage of 0.9% FA in water (A). The flow rate was 0.2 mL·min⁻¹ and the column was kept at 30°C. The sample injection volume was 1 µL. The data were acquired using Xcalibur software v.4.0.27.19 (Thermo Scientific). The method consisted of several cycles of full MS scans (*R* = 70,000; scan range = 75–1125 *m/z*) followed by three ddMS2 scans (*R* = 17,500; 20, 40, 60 NCE) in negative mode. External calibration was performed using LTQ ESI negative ion calibration solution (Thermo Scientific). The generated mass spectra were processed using Compound Discoverer 3.2 (Thermo Scientific) for small molecule identification.

Nuclear magnetic resonance spectroscopy

Ethyl acetate extracts were dried under a soft nitrogen flow (approx. 5 mg) and solubilized in 500 µL of DMSO-*d*₆ for NMR analyses. All NMR spectra (¹H, ¹H–¹H COSY, ¹H–¹³C HSQC, ¹H–¹³C HMBC) were acquired at 25°C using an Avance III 800 CRYO spectrometer (Bruker Biospin, Rheinstetten, Germany) in 5-mm-diameter NMR tubes. MestReNova, Version 11.04–18,998 (Mestrelab Research, S.L.) was used to process the raw data.

Transcriptome analysis

Total RNA extraction of liquid-grown mycelia was performed essentially as previously described (Hartmann et al., 2015) using a TissueLyser LT (Qiagen) for cell

disruption. The quality and quantity of RNA were determined by capillary electrophoresis using an HS RNA kit and 5200 Fragment Analyser (Agilent). For single-end RNA sequencing (RNA-seq), libraries were generated using the Smart-Seq2® mRNA assay (Illumina, Inc.) according to the manufacturer's instructions. Samples were indexed and sequenced on the Illumina NextSeq550 (20M reads *per* sample). Generated FastQ files were analysed with FastQC and any low-quality reads were trimmed with Trimmomatic (Bolger et al., 2014). All libraries were aligned to *A. terreus* NIH2624 genome assembly (ASM14961.v1) with gene annotations (built 2010-06) from Ensembl Fungi using HISAT2 v. 2.2.1 (Kim et al., 2015) with sensitive option and maximum intron length at 4000. Read counts were obtained using featureCounts v2.0.1 (Liao et al., 2014). All RNA-seq experiments were carried out in three biological replicates. Differential expression analysis was performed using DESeq2 v.1.24.0 (Love et al., 2014). Transcript abundance was defined as transcripts *per* million (TPM). The genes that showed more than log₂ 1-fold expression changes and above median TPM with adjusted *p*-value < 0.05 are defined as significantly differentially expressed genes in this analysis.

Two strategies were implemented to identify upregulated genes that were absent or incorrectly annotated in the current *A. terreus* NIH2624 genome assembly. To identify genes that could be incorrectly joined together in the annotation, the differentially expressed exons were determined as described above for gene features. Genes that showed simultaneously up- and downregulated exons were manually curated. To identify genes that were not in the current annotation, the entire genome was divided into 500 bp length sections, which were analysed as described above as if they were genes/exons. The upregulated differentially expressed sections (threshold set for upper quartile expression levels) not attributed to a currently annotated gene were manually curated. Automated gene structure prediction of new genes or poorly annotated genes was done using AUGUSTUS (Hoff & Stanke, 2013). Gene structure was manually curated according to RNA-seq data and used in the transcriptome analysis (Table S2).

Protein domain entries were obtained from InterPro 90.0 either from predetermined data or using InterProScan (REST) service to search entries for the new gene predictions (Paysan-Lafosse et al., 2023). The enrichment analyses were performed with the FunRich software v.3.1.3 (Pathan et al., 2017), with a *p*-value < 0.05 after Bonferroni correction. Functional characterization and metabolic pathway analysis was performed using the KEGG application KofamKoala (Aramaki et al., 2020). Metabolic gene clusters were identified within annotated genomes (GenBank or RefSeq) through sequence homology searches using cblaster v.1.3.12 (Gilchrist et al., 2021) using default filtering thresholds.

Reverse transcription–quantitative PCR analysis (RT-qPCR)

Total RNA was extracted as reported above, and cDNA synthesis followed a previously described protocol (Hartmann et al., 2015). Oligonucleotide pairs were designed using Primer-BLAST (Ye et al., 2012) and supplied by STAB Vida (Oeiras, Portugal) (Table S3). The RT-qPCR analysis was performed in a CFX96 Thermal Cycler (Bio-Rad) using the SsoFast EvaGreen Supermix (Bio-Rad), 250 nM of each oligonucleotide and the cDNA template equivalent to 10 ng of total RNA, at a final volume of 10 μ L per well, in three biological replicates. The PCR conditions were: enzyme activation at 95°C for 30 s; 40 cycles of denaturation at 95°C for 5 s and annealing/extension at 60°C for 15 s and a melting curve obtained from 65°C to 95°C, consisting of 0.5°C increments for 5 s. Data analyses were performed using the CFX Manager software v.3.1 (Bio-Rad). The expression of each gene was taken as the relative expression in pair-wise comparisons of each condition relative to the acetate control. The expression of all target genes was normalized by the expression of the gamma-actin gene ATEG_06973 or AN6542.

Generation of gene replacement mutants

The genes AN0331, *hmgA* (AN1897), AN4576, AN10530 and AN12484 were selected for gene replacement with *A. fumigatus pyrG* in *A. nidulans* A1149 strain, performed according to a well-established method (Szewczyk et al., 2007), essentially as previously described (Martins et al., 2015). Oligonucleotides were designed as described above (Table S3). Gene replacement was confirmed by PCR (Figure S1).

RESULTS

During gallate catabolism in *Aspergillus terreus*, the 3-oxoadipate and homogentisate central pathways are mostly unregulated

A comparative transcriptome analysis was performed here aiming to disclose the central pathways relevant to the catabolism of gallate in *A. terreus*. During gallate catabolism (approx. 30% consumed of 20 mM), 1545 encoding genes were found differentially upregulated and 1756 downregulated (see Figure S2 for principal component analysis and MA plots, and Table S4). Functional analysis of differentially expressed genes revealed that the global response to gallate in comparison with the control acetate differed in the regulation mechanisms (Figure S3A,B). Gallate-induced response mainly occurs at the transcriptional regulation, and resorts more to fungi-specific DNA binding transcription factors (IPR036864). On the contrary, acetate-induced response apparently occurs more at the translational and post-translational regulation and involves proteins containing RNA binding/modifying domains (IPR012340, IPR012677, IPR001412, IPR014729, IPR009000) and proteasome degradation domains (IPR001353, IPR029055, IPR023332). This may, however, be biased since more is unknown in the upregulated genes dataset. About 21% of upregulated genes do not have a known protein domain in comparison with only ca. 10% in the control (17.6% in all genes). Moreover, 72% of upregulated genes are currently not functionally annotated using KEGG, while only 36% of the downregulated ones are not. The major facilitator superfamily (MFS) of transporters (IPR036259) was 2-fold enriched and represented 8% of all upregulated genes. The general response to gallate is relatively

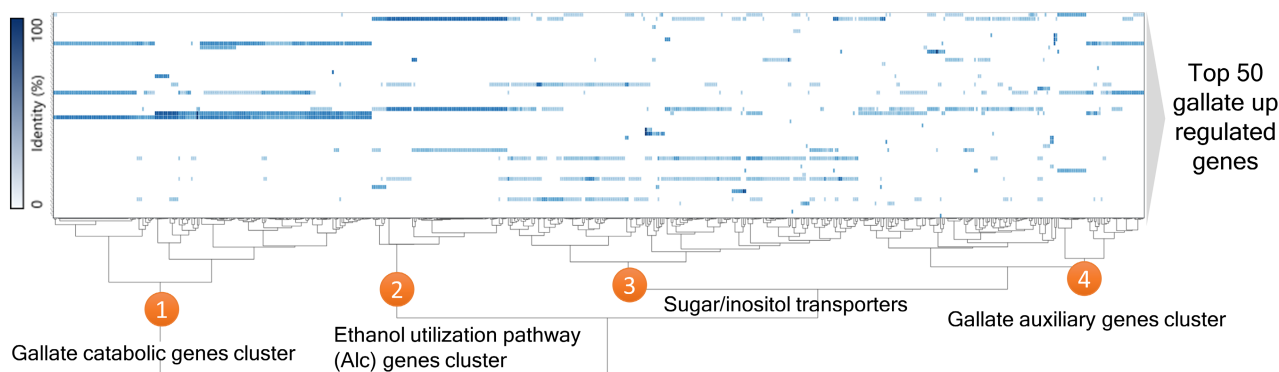


FIGURE 2 Gene cluster analysis with the top 50 most abundant genes (TPM) differentially upregulated (Fold Change >2) in response to gallate in *A. terreus*. Co-localized genes were identified within RefSeq annotated fungal genomes through sequence homology searches, and their hierarchical clustering analysis was done using the program cblaster (603 clusters across 578 genomic scaffolds from 375 organisms were detected; see also Table S6). Four main clusters were observed including one containing the four catabolic genes of the gallate pathway.

FIGURE 3 Gallate and related gene clusters identified in Ascomycota fungi. Here are depicted selected examples of the three main gene cluster types having a distinct flavoprotein monooxygenase as a core gene (highlighted by the *Aspergillus terreus* genes ATEG_05726b, ATEG_08220 and ATEG_08831). These gene clusters additionally often include a fumarylacetoacetate hydrolase (FAH)-like gene (ATEG_04856), a DUF3500 gene (ATEG_08221-22) and a fungal conserved short protein with no known domains' gene (ATEG_04855) alongside with transporter (MFS) and transcription factor genes. Clusters were identified within RefSeq annotated fungal genomes through sequence homology searches and graphical representation using the programs cblaster and clinker respectively. Homologous genes are represented using a colour code and gene links represent an identity threshold of over 30%. The locus accession number is given below the species name and the asterisk indicates a gene with a new structure annotation.

similar to that towards salicylate (e.g. enriched protein domain families; Martins et al., 2021), except for the secondary metabolism which is mostly unregulated in gallate but upregulated in salicylate.

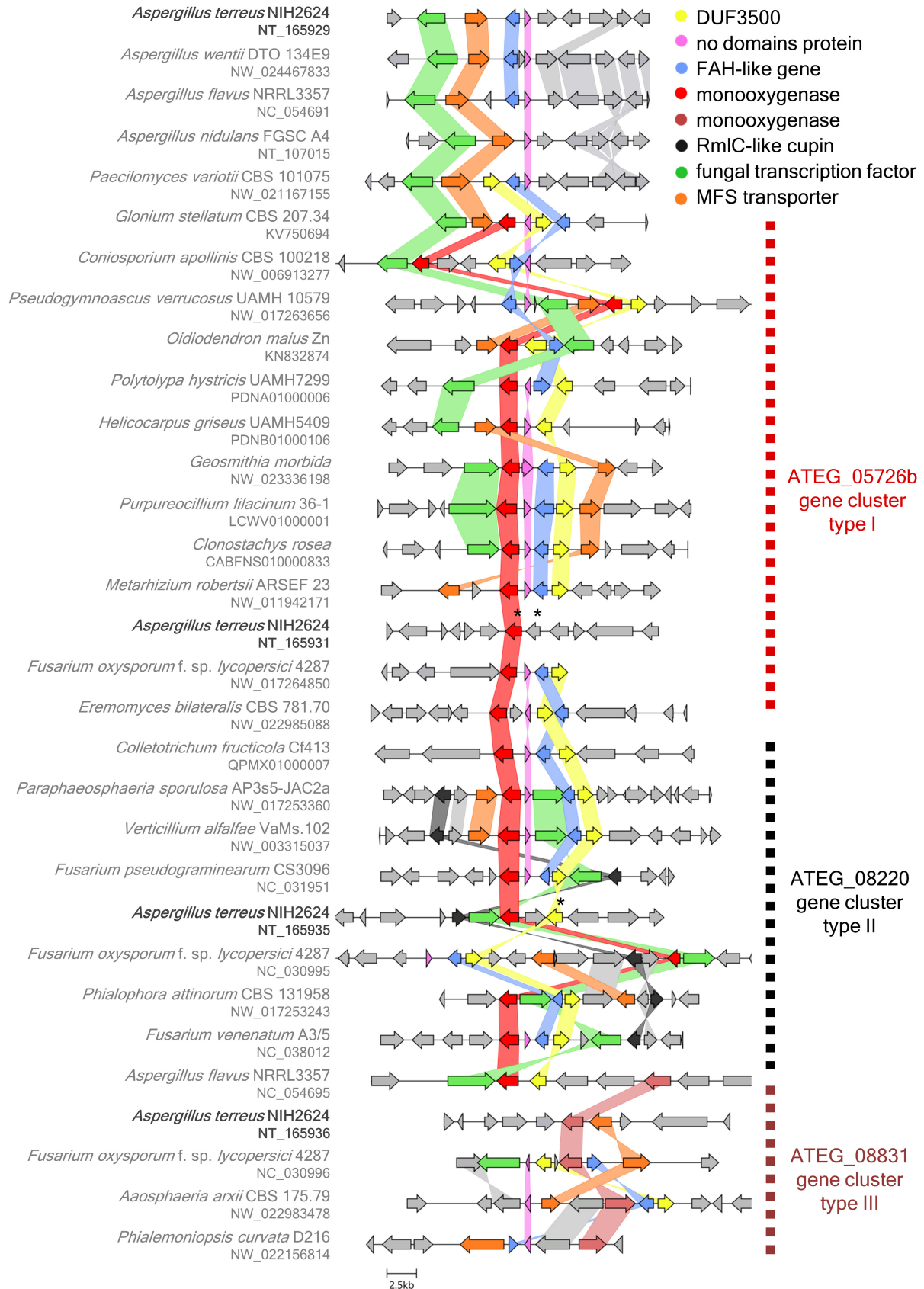
The known central pathways, namely, the 3-oxoadipate, the homogentisate and the 3-hydroxyanthranilate pathways for the catabolism of aromatic hydrocarbons were either unregulated or showed upregulation with moderate transcripts abundance (Table S5). The 3-oxoadipate pathway was globally the central pathway most responsive to gallate, especially the protocatechuate branch (Table S5). Quinate or shikimate catabolism (or hypothetically from an initial reduction of gallate) via protocatechuate is dependent on *qutC* (ATEG_00348), 3-dehydroshikimate dehydratase, which mediates the reaction that connects the upper and the central catabolic pathways (e.g. protocatechuate branch), intersecting also with the anabolic shikimate pathway (Hawkins et al., 1993). The predicted quinate utilization cluster (ATEG_00348 to ATEG_00355), including *qutC*, was scarcely expressed. Similarly, a second quinate utilization-like cluster (ATEG_07672_new to ATEG_07676), not present in, e.g., *A. nidulans*, was also scarcely expressed (Table S5). Other *qutC* homologues were unregulated, nearly excluding a path of initial reduction of gallate. Moreover, as previously reported for *A. niger* (Boschloo et al., 1990), we also observed that the protocatechuate branch is not essential for the catabolism of gallate in *A. nidulans* (see below).

Four genes compose the gallate catabolic pathway in *Aspergillus terreus*

The transcriptional reprogramming induced by gallate was confirmed by the upregulation and very high expression of several tannase genes: ATEG_02651 orthologue of AO090023000047 (Koseki et al., 2018), ATEG_03047 orthologue of An18g03570 (Ramírez-Coronel et al., 2003) and ATEG_07937 orthologue of AO090103000074 (Hatamoto et al., 1996). This was anticipated since gallate, found in tannic acid comprising esters of polygalloylglucose or polygalloylquinic acid, is known as an inducer of tannase activity (Arentshorst et al., 2021; Mäkelä et al., 2015). The tannic acid transcriptional activator-repressor module composed of *tanR* (ATEG_10383) and *tanX* (ATEG_10381) (Arentshorst et al., 2021) was also found to be upregulated though more modestly expressed. Additional esterase genes

(ATEG_08115b_new and ATEG_09944) and *O*-methyltransferases (ATEG_07862, ATEG_09300 and ATEG_01928) were also highly expressed and upregulated, suggestive of a role in the metabolism of esters of gallate or their precursors (Table S5).

Some gene clusters of upregulated genes were identified but none contained the abovementioned tannases, esterases and *O*-methyltransferases. The central pathways for the catabolism of aromatic compounds are every so often organized into clusters of genes in the genomes of fungi (Martins et al., 2019). The hypothesis that some gallate upregulated genes in *A. terreus* are in a gene cluster in other species was tested using the top 50 abundant transcripts with an FC > 2 (Figure 2; similar results were obtained using the top 100). Four hierarchical groups of gene clusters were identified; these comprise (i) sugar/inositol transporters genes (IPR003663), (ii) genes of the ethanol utilization pathway (discussed below), (iii) gallate metabolism auxiliary genes and (iv) four genes, including a putative monooxygenase and a fumarylacetoacetate hydrolase (FAH)-like gene—hallmarks of a catabolic gene cluster of aromatic compounds. Further analysis of the last main hierarchical group (iv) revealed that three gene cluster's types, each having a distinct flavoprotein monooxygenase (CATH code 3.50.50.60, prototype reaction—aromatic hydroxylation, Paul et al., 2021) as a core gene, are present across species of Ascomycota (Figure 3) and only one in Basidiomycota (Figure S4). The genes of the three cluster types are in four loci in the genome of *A. terreus*, and four of them are highly expressed and upregulated (ATEG_04855, ATEG_04856, ATEG_05726b_new and ATEG_08221-22_new; hereafter denominated the four catabolic genes of the gallate pathway) (Table S5). Two of the three flavoprotein monooxygenase genes were found upregulated, though ATEG_05726b_new was more highly expressed. The encoded protein of the *A. niger* orthologue (NRRL3_4659), can convert in vitro protocatechuate in 1,2,4-trihydroxybenzene (hydroxyquinol), hence recently suggested to convert gallate to 1,2,3,5-tetrahydroxybenzene (Lubbers et al., 2021). The other highly expressed genes present in the three types of clusters are a FAH-like (ATEG_04856), a fungal conserved short protein gene (ATEG_04855) with no known domains (containing a conserved nucleophilic residue serine, a.a. 64, and only found in Dykaria) and a domain of unknown function DUF3500 gene (ATEG_08221-22_new) that currently remains uncharacterized. The last two genes



do not have any homologues in the genome, while the FAH-like gene has eight homologues, although none of them upregulated. In bacteria, DUF3500 genes

are also often located adjacent or in the vicinity of an FAH-like gene not closely related to the characterized ones (data not shown). They are mostly only present in

FCB, Proteobacteria, PVC and Terrabacteria groups, and Acidobacteriota phylum. Finally, in fungi, DUF3500 genes are mostly found in filamentous Ascomycota (i.e. Pezizomycotina subphylum) and Basidiomycota with macroscopic fruiting bodies (i.e. Agaricomycotina subphylum) (Paysan-Lafosse et al., 2023).

The massive expression and upregulation of the ethanol utilization pathway (Table S5) constituted of alcohol dehydrogenase *alcA* (ATEG_09407 orthologue of *alcA/AN8979*), aldehyde dehydrogenase *aldA* (ATEG_05020 orthologue of *aldA/AN0554*) and transporter *alcS1* (ATEG_03626-27_new; with homology to *alcS/AN8981* and *AN8390*; Flipphi et al., 2009) strongly indicate the production of their physiological inducer acetaldehyde (Flipphi et al., 2009). The regulator ATEG_03627 with homology to *alcR/AN8978* was also positively regulated. Acetaldehyde can be produced from the catabolism of compounds as diverse as ethanol, amino acid threonine, catechol (meta-cleavage) or phenylpropionic acids (aka hydroxycinnamic acids). Cytosolic pyruvate carboxylase *pycA* (ATEG_05433) was found to be upregulated, most likely contributing to the formation of acetaldehyde and induction of the ethanol utilization pathway. Additionally, *acuA* (acetyl-CoA synthetase), *acuC* (transcriptional activator) and *cpA* (transport of acetate ions with homology to *alcS*) were upregulated despite the control condition acetate.

The four catabolic genes of the gallate pathway, but not the ethanol utilization pathway, were also found here upregulated in *A. flavus* in the presence of gallate, notwithstanding the co-metabolic conditions used in this previous study (Zhao et al., 2018).

The four catabolic genes of the gallate pathway are essential for gallate utilization in *Aspergillus*

The gallate-induced transcriptional response suggests that the main catabolic pathway for gallate in *A. terreus* starts with initial hydroxylation (decarboxylating) and formation of the central intermediate 1,2,3,5-tetrahydroxybenzene. Processing of this intermediate through the central pathway results in the build-up of end metabolites that trigger the induction of the ethanol utilization pathway and C2 metabolism. To confirm this hypothesis using gene deletion mutants, our option was to resort to *A. nidulans* for which a commercial strain capable of efficient recombination is readily available. Gene expression analysis first validated the results obtained in RNA-seq of *A. terreus* (Figure 4A). Importantly, a similar gene regulation was observed for *A. nidulans*: the highly conserved orthologues of the four catabolic genes of the gallate pathway were upregulated (Figure 4B). None are in close vicinity to each other in the genome, despite synteny of the AN0331 loci with other aspergilli (Figure 3). These four genes showed a remarkable

induction from the early culture timepoints in both aspergilli, in opposition to the other genes of the central pathways analysed. These results mostly verify that the same pathway is used in both species, furthering its relevance across aspergilli.

Based on these results, gene functional assays were performed using the four catabolic gene deletion mutants in *A. nidulans*. These mutants showed severely impaired growth in gallate and tannic acid solid media (Figure 5) demonstrating their essential role in the catabolism of gallate. Growth of deletion mutants in other aromatic compounds, namely, 2,3-dihydroxybenzoate, phenylacetate, phloroglucinol, protocatechuate and resorcinol was unaffected (Figure 5 and Figure S5). This revealed that the four catabolic genes are most likely only essential to the catabolism of gallate and other compounds that share the same central pathway unrelated to those previously described. Growth in an isomer of gallate, 2,4,6-trihydroxybenzoate, showed severe growth impairments like those imposed by gallate, except for the monooxygenase deletion mutant (Δ AN4576). This indicated that the central metabolite 1,2,3,5-tetrahydroxybenzene was formed through hydroxylation (decarboxylating) of gallate and its isomer.

1,2,3,5-Tetrahydroxybenzene is the central intermediate of the gallate catabolic pathway in *Aspergillus*

To further validate 1,2,3,5-tetrahydroxybenzene as a new central intermediate, the metabolites accumulating after the addition of gallate or its isomer to acetate pre-grown cultures of *A. nidulans* gene deletion mutants were analysed. Although the consumption rate of gallate seemed to be highly reduced, neither gallate nor its metabolites accumulated in incubations of the Δ gallate 1-monooxygenase (Δ AN4576), suggestive of functional redundancy (Figures S6 and S7A,B). Transient accumulation of 1,2,3,5-tetrahydroxybenzene in cultures of gallate and its isomer was observed for the Δ DUF3500 gene (Δ AN10530) only in the presence of supplemented ascorbic acid (Figure 6, see confirmation on the synthesis in Figure S8A,B), likely because it prevented autooxidation from occurring. 1,2,3,5-tetrahydroxybenzene was also shown to be unstable in phosphate buffer even at low pH. The resulting autooxidation metabolites were mostly not identified by GC–MS except for 2-furoic acid (Figure 6 and Figure S9). Accumulation of a single compound was detected in Δ no domains short protein (Δ AN0331); identified as 5-hydroxydienelactone based on NMR and mass spectral data (Figures 6 and 7 and Figure S10). For the Δ FAH-like gene (Δ AN12484), the transient accumulations of a major unidentified compound (calculated MW 223.04795 and putative formula $C_{10}H_9NO_5$ by LC–MS; non-aromatic by NMR; resolved as three analytes with the same molecular ion by GC after derivatization) and

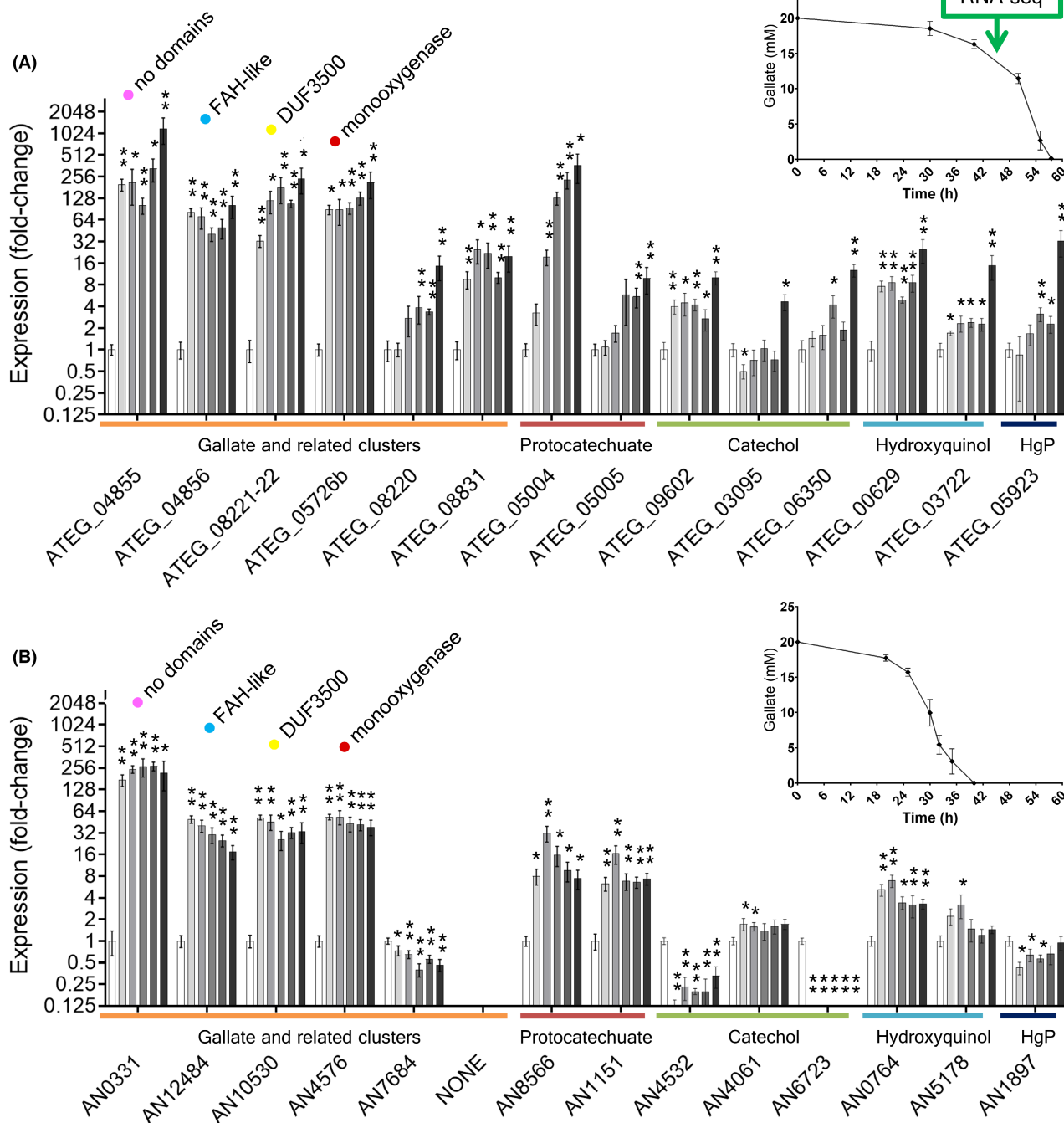


FIGURE 4 Gene expression of the gallate pathway genes and other central pathways of *Aspergillus terreus* (panel A) and the respective *A. nidulans* orthologues (panel B) along the time of cultivation in gallate media (grey bars) compared to the control in acetate media (white bar). The distinct monoxygenase types from gallate-like gene clusters are also shown. Representative genes of the 3-oxoadipate pathway (protocatechuate and catechol branches and the hydroxyquinol variant) and the homogentisate pathway (HgP) were chosen including the respective dioxygenase gene. The five timepoints for gene expression in gallate media correspond to those depicted in the graphical inserts for the consumption of gallate, except for the first (0h) and the last: 30, 40, 44 (RNA-seq assay timepoint), 50 and 55h for *A. terreus*; 20, 25, 30, 32 and 35h for *A. nidulans*. In acetate media, 40 and 35h, respectively, for *A. terreus* and *A. nidulans* (**p*-value <0.05; ***p*-value <0.005).

some other metabolites including acetopyruvate were noticed (Figure 6, Figures S11 and S12 and Table S7). FAH is a diversified superfamily of proteins (IPR011234) with catalytic functions of hydrolase, lyase and isomerase (Weiss et al., 2018). The nature of the molecule that

transiently accumulated in cultures of this gene deletion mutant remains unresolved. It is also not possible to state whether it is a direct or indirect product, the latter being the result of redundant enzymatic activities. However, it may be hydrolysed to form, at least non-specifically,

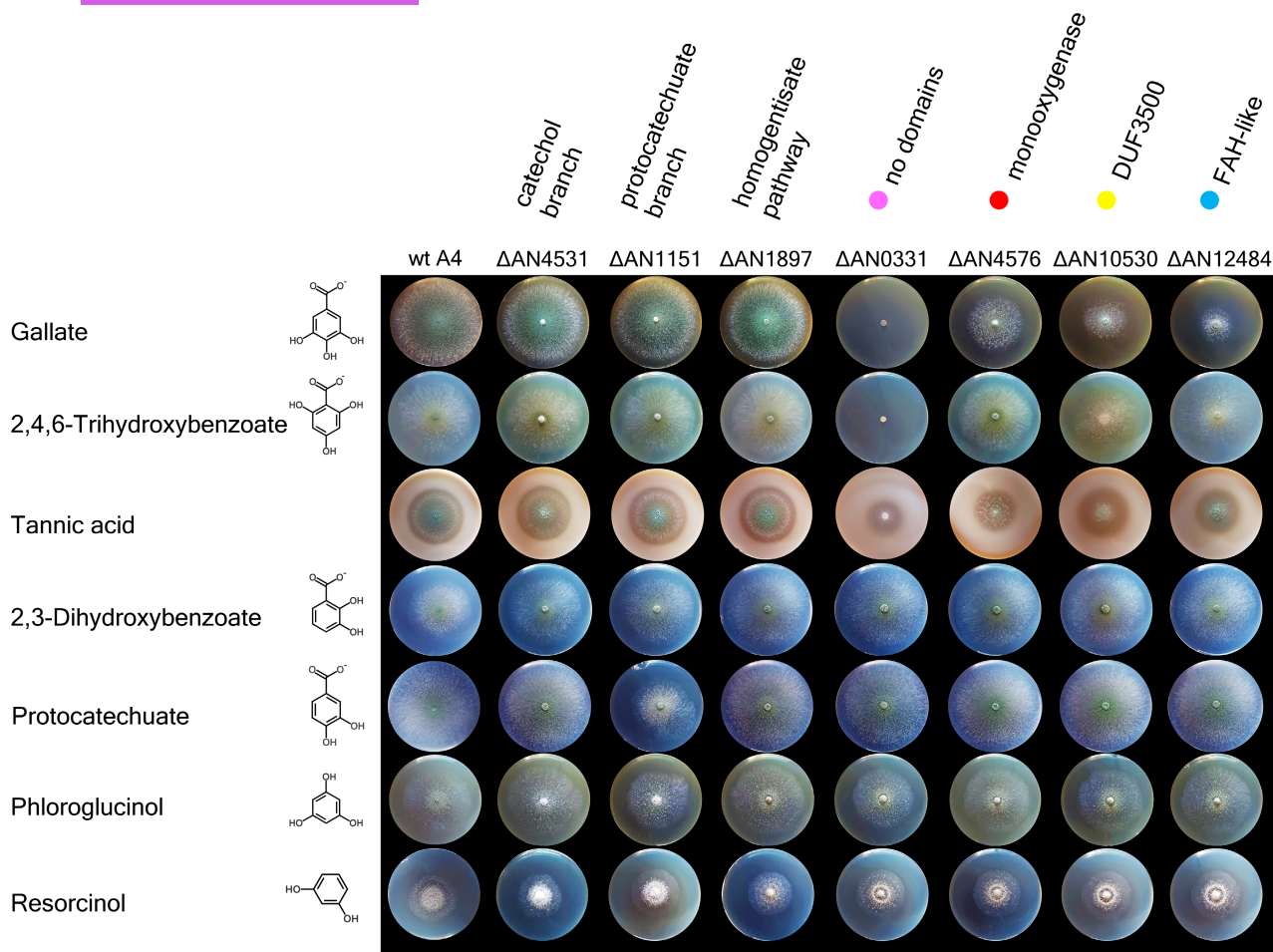


FIGURE 5 *Aspergillus nidulans* wild-type and gene deletion mutants grown in gallate and other carbon sources. Mutant strains of the four gallate pathway genes showed phenotypes of growth impairment for gallate, its isomer 2,4,6-trihydroxybenzoate (except for Δ AN4576) and tannic acid utilization as a carbon source. Δ AN10530 growth media also accumulated a coloured metabolite for gallate or related compounds. The mutants used as control, namely, of the catechol branch or protocatechuate branch of the 3-oxoadipate pathway, and homogentisate pathway showed the expected growth phenotypes in the respective metabolites of their pathways, i.e., normal growth for Δ AN4531 in 2,3-dihydroxybenzoate, growth impairment for Δ AN1151 in protocatechuate (note: phenylacetate was a very poor carbon source for all strains at the low pH used). Aromatic hydrocarbons (20 mM) or tannic acid (2.5 mM) were added as the main carbon source to solid minimal media (pH5.0).

acetopyruvate or a reduced form (putative 2-hydroxy-4-oxopentanoic acid) as these were only identified in Δ FAH-like cultivations (Figure S11).

In summary, the proposed pathway starts with an initial hydroxylation (decarboxylating) step, which is followed by ring-cleavage (di)oxygenation and immediate (spontaneous) cyclization to create 5-hydroxydienelactone. This compound is then activated to form a resulting nitrogenous adduct and ultimately hydrolysed to produce acetopyruvate or its reduced form (Figure 8).

DISCUSSION

In this study, we report the discovery of a novel central pathway in fungi responsible for the catabolism of gallate and related aromatic compounds using the central intermediate 1,2,3,5-tetrahydroxybenzene (Figure 8).

Surprisingly, this pathway differs from those described and/or proposed before for the catabolism of gallate in both bacteria and fungi (Lubbers et al., 2019). Based on this discovery, it is wrong to refer to gallate as a central metabolite for fungi; instead, gallate is one of several compounds channelled towards this novel central pathway. The pathway contains two genes encoding proteins having yet no known activities (i.e. DUF3500 and no domains short protein), which necessitates further investigation into their unusual mechanisms of action. However, based on the data, we hypothesize that the DUF3500 protein functions as a newly discovered ring-cleavage enzyme, deserving focused analysis soon.

The intermediate 1,2,3,5-tetrahydroxybenzene was previously reported in the catabolism of aromatic compounds in bacteria, specifically in the catabolism of gallate or phloroglucinol. It functions as a cocatalyst in the anaerobic conversion of pyrogallol

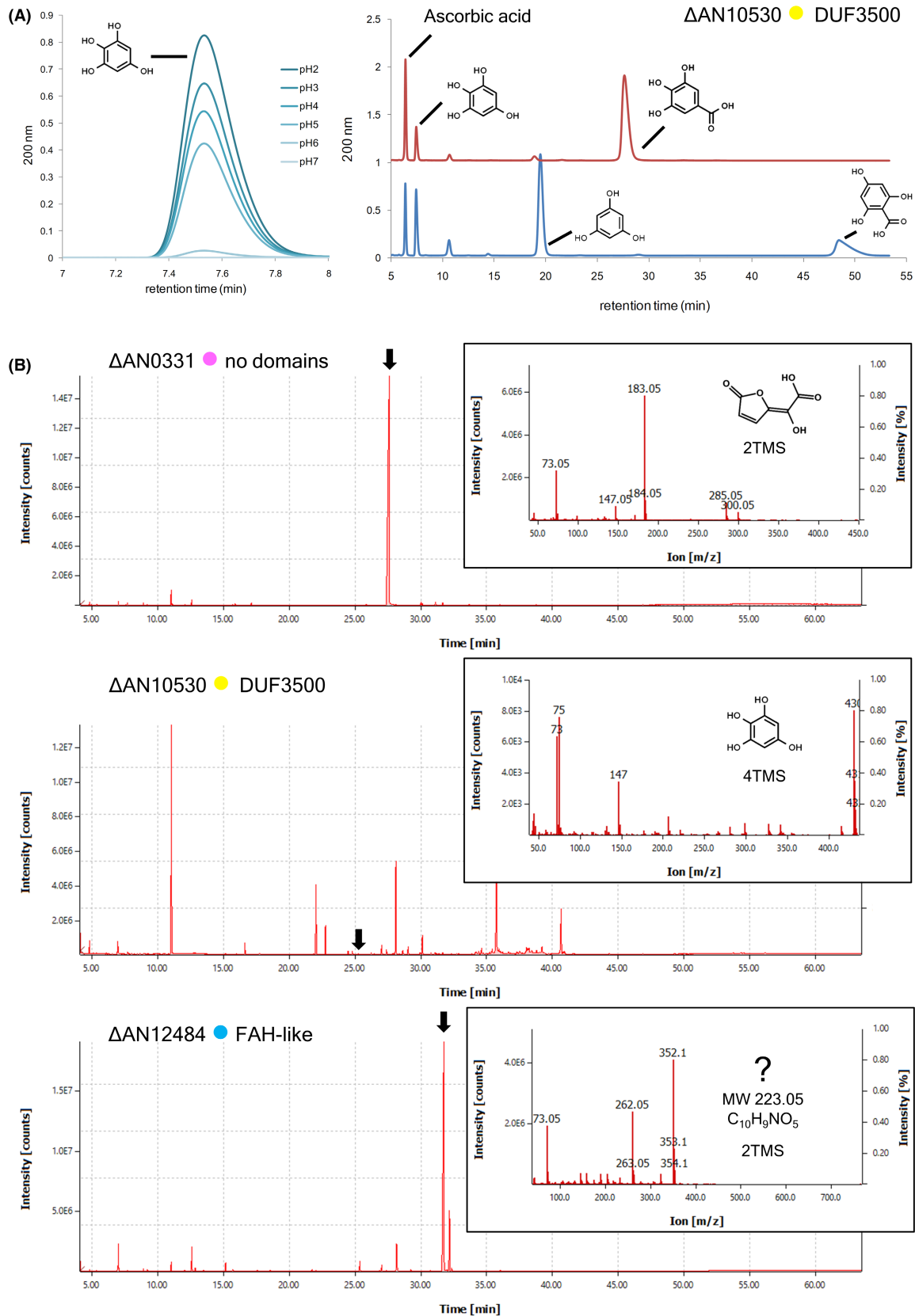


FIGURE 6 Gallate-derived metabolites differentially accumulated in cultures of the four catabolic gene deletion mutants. HPLC chromatograms (panel A) of 1,2,3,5-tetrahydroxybenzene in different pH (10-mM potassium phosphate buffer) for 30 min (left side) and its accumulation in Δ AN10530-DUF3500 cultures (16h, pH3.0) in the presence of ascorbic acid from either gallate or its isomer 2,4,6-trihydroxybenzoate (right side; HPLC method B). GC-MS chromatograms (panel B) for the respective gene replacement mutants' culture extracts and the mass spectrum of selected analyte molecules (indicated by an arrow).

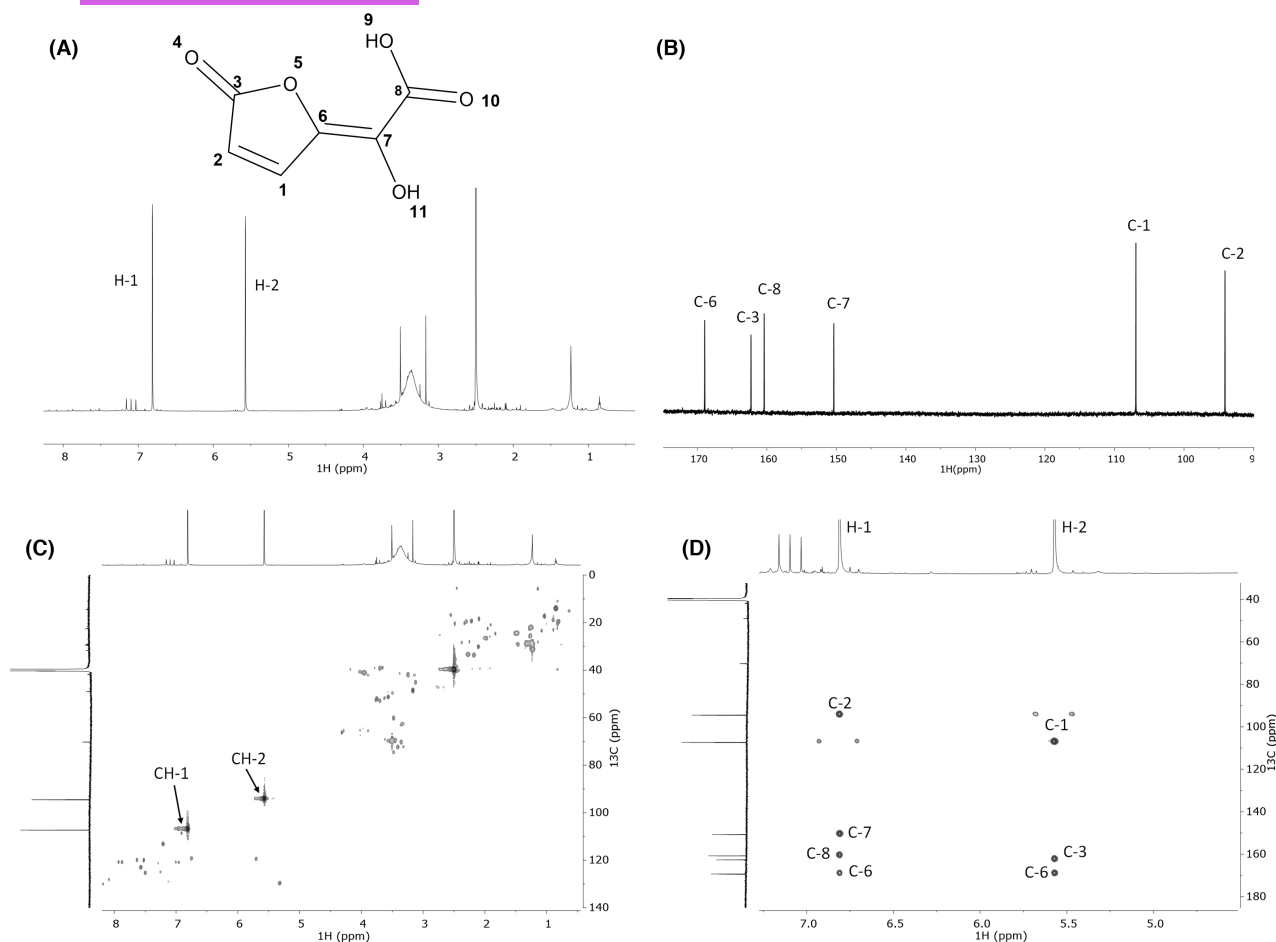


FIGURE 7 Wide-ranging NMR spectral characterization of Δ AN0331 sample extract with the assignment of the signals related to the presence of 5-hydroxydienelactone. The ¹H NMR (A); The ¹³C NMR (B); the ¹H-¹³C HSQC spectrum (C) and the ¹H-¹³C HMBC spectrum (D). 5-hydroxydienelactone: ¹H NMR (800 MHz, DMSO-d₆): 5.57 (d, J=2.2 Hz, 1H); 6.81 (d, J=2.2 Hz, 1H); ¹³C NMR (201 MHz, DMSO-d₆): 94.11; 106.92; 150.37; 160.38; 162.28; 168.93.

to phloroglucinol, i.e., after initial non-oxidative decarboxylation of gallate (Paizs et al., 2007), or as a hydroxylation intermediate in the catabolism of phloroglucinol (Armstrong & Patel, 1993). Only the last partially resembles the central pathway reported here, as acetylpyruvate was also identified as a near-end-metabolite. They, however, may differ, because in the bacteria phloroglucinol catabolism proceeds through this pathway but this dependence was not observed here in *A. nidulans* (Figure 5). In a recent study, the derivative 6-methoxy-1,2,4-trihydroxybenzene (6-MeOTHB) of the central intermediate 1,2,3,5-tetrahydroxybenzene was identified during the catabolism of syringate (also a methoxy derivative of gallate) in the Basidiomycota *Phanerochaete chrysosporium* (Kato et al., 2022). 6-MeOTHB was converted in vitro, by hydroxyquinol 1,2-dioxygenase, to 4-hydroxy-2-methoxy-*cis*, *cis*-muconate (Kato et al., 2022) but the subsequent catabolic steps were unlooked. Syringate can be metabolized into 5-hydroxyvanillate (Kato et al., 2022; Lubbers et al., 2019), which likely undergoes prompt

conversion to either 6-MeOTHB or 1,2,3,5-tetrahydroxybenzene, thereby effectively excluding the formation of gallate. The DUF3500 and the no domains short protein genes are both absent in *Phanerochaete* genomes, despite being present in genomes of various species in the subphylum Agaricomycotina. These findings suggest that additional pathways for the metabolism of 1,2,3,5-tetrahydroxybenzene or its methoxy derivatives await discovery. Finally, the DUF3500 gene is well represented in certain bacteria genomes, including, for example, *Sphingomonas*, where it may explain the redundancy observed in this bacteria; deletion of the known key gallate catabolic genes—LigAB (protocatechuate 4,5-dioxygenase), DesZ (3-O-methylgallate 3,4-dioxygenase) and DesB (gallate dioxygenase)—did not block gallate utilization (Kasai et al., 2007).

The newly discovered 1,2,3,5-tetrahydroxybenzene central pathway is common in certain subphyla of fungi (i.e. those comprising the DUF3500 gene) and likely plays a significant role in the breakdown of aromatics, particularly those derived from

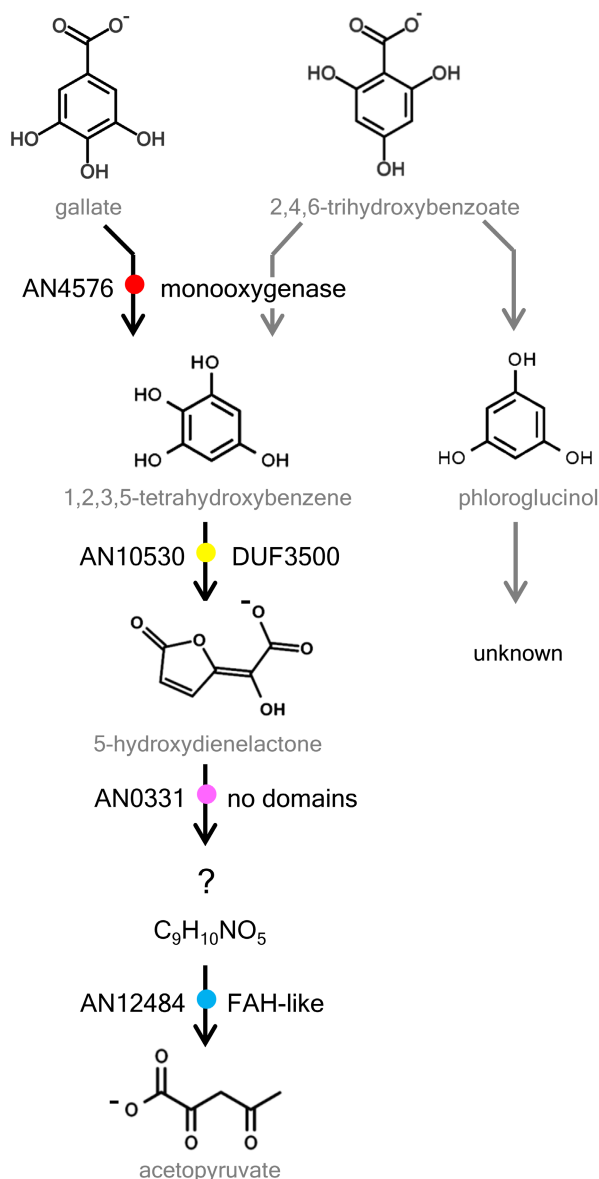


FIGURE 8 The proposed gallate and related aromatic compound catabolic pathway through the central intermediate 1,2,3,5-tetrahydroxybenzene. The grey arrows denote reactions that lack current gene annotations.

syringyl-rich lignin, including gallate and related compounds. These findings surely expand the current understanding of the toolkit of central pathways for the catabolism of aromatic compounds in fungi. Besides, it questions the accuracy of the generalized (yet unproven) assumption that gallate catabolism depends on the previously known five main central pathways. This novel central pathway has great ecological and biotechnological importance, not only for fungi but also potentially for bacteria. The lignin found in various economically significant plants, such as major grains like rice, wheat and maize, comprises a substantial portion of syringyl units (up to 60%). As a result, the future utilization of residues from these plants in biorefineries will

yield significant quantities of syringyl derivatives. Therefore, the information on the new central pathway is crucial for comprehensive studies on the degradation of complex polymers like lignin and surely may impact the development of technologies aimed at deconstructing and converting them into added-value chemicals.

AUTHOR CONTRIBUTIONS

Tiago M. Martins: Conceptualization (lead); formal analysis (equal); investigation (lead); methodology (lead); writing – original draft (lead). **Artur Bento:** Investigation (equal). **Celso Martins:** Investigation (equal). **Ana S. Tomé:** Investigation (equal). **Carlos J. S. Moreira:** Investigation (equal). **Cristina Silva Pereira:** Conceptualization (equal); project administration (equal); resources (equal); supervision (equal); writing – review and editing (equal).

ACKNOWLEDGEMENTS

The authors are grateful to Maria C. Leitão (ITQB-NOVA Small Molecules Analysis) for the implementation and support in the chromatographic analyses. Mass spectrometry data were generated by the Mass Spectrometry Unit (UniMS), ITQB/iBET, Oeiras, Portugal. All members of the Silva Pereira lab are also thanked for useful discussions.

FUNDING INFORMATION

This work was financially supported by National Funds from Portugal2020 and FEDER under the project “BIOPINUS” (Ref. 13/SI/2020-072630) and through Fundação para a Ciência e a Tecnologia (FCT) through MOSTMICRO-ITQB R&D Unit (UIDB/04612/2020, UIDP/04612/2020) and LS4FUTURE Associated Laboratory (LA/P/0087/2020). TM and CM are grateful to FCT for the working contract financed by National Funds under Norma Transitória D.L. n.º 57/2016 and the Fellowship SFRH/BD/118377/2016 respectively. The NMR data were acquired at CERMAX, ITQB-NOVA, Oeiras, Portugal with equipment funded by FCT.

CONFLICT OF INTEREST STATEMENT

The authors declare that they have no competing interests.

DATA AVAILABILITY STATEMENT

All relevant data are available in the manuscript. Supplementary figures and tables are provided to support the results presented in this manuscript. Gene transcript TPM values are contained in Table S4, and raw data with metadata were deposited in the Sequence Read Archive under Bioproject accession number PRJNA612036.

ETHICS STATEMENT

Not applicable.

ORCID

Tiago M. Martins  <https://orcid.org/0000-0003-1474-9971>

Artur Bento  <https://orcid.org/0000-0003-4097-1613>

Celso Martins  <https://orcid.org/0000-0002-8269-9550>

Ana S. Tomé  <https://orcid.org/0000-0002-5152-7908>

Carlos J. S. Moreira  <https://orcid.org/0000-0002-7708-2505>

Cristina Silva Pereira  <https://orcid.org/0000-0002-6750-1593>

REFERENCES

- Aramaki, T., Blanc-Mathieu, R., Endo, H., Ohkubo, K., Kanehisa, M., Goto, S. et al. (2020) KofamKOALA: KEGG ortholog assignment based on profile HMM and adaptive score threshold. *Bioinformatics*, 36, 2251–2252.
- Arentshorst, M., Falco, M.D., Moisan, M.-C., Reid, I.D., Spaapen, T.O.M., van Dam, J. et al. (2021) Identification of a conserved transcriptional activator-repressor module controlling the expression of genes involved in tannic acid degradation and gallic acid utilization in *Aspergillus niger*. *Frontiers in Fungal Biology*, 2.
- Armstrong, S. & Patel, T. (1993) 1,3,5-trihydroxybenzene biodegradation by *Rhodococcus* sp. BPG-8. *Canadian Journal of Microbiology*, 39, 175–179.
- Bolger, A.M., Lohse, M. & Usadel, B. (2014) Trimmomatic: a flexible trimmer for Illumina sequence data. *Bioinformatics*, 30, 2114–2120.
- Boschloo, J.G., Paffen, A., Koot, T., Vandentweel, W.J.J., Vangorcom, R.F.M., Cordewener, J.H.G. et al. (1990) Genetic analysis of benzoate metabolism in *Aspergillus niger*. *Applied Microbiology and Biotechnology*, 34, 225–228.
- Ferrer-Sevillano, F. & Fernandez-Canon, J.M. (2007) Novel *phacB*-encoded cytochrome P450 monooxygenase from *Aspergillus nidulans* with 3-hydroxyphenylacetate 6-hydroxylase and 3,4-dihydroxyphenylacetate 6-hydroxylase activities. *Eukaryotic Cell*, 6, 514–520.
- Flippi, M., Sun, J., Robellet, X., Karaffa, L., Fekete, E., Zeng, A.-P. et al. (2009) Biodiversity and evolution of primary carbon metabolism in *Aspergillus nidulans* and other *Aspergillus* spp. *Fungal Genetics and Biology*, 46, S19–S44.
- Gérecová, G., Neboháčová, M., Zeman, I., Pryszyk, L.P., Tomáška, L., Gabaldón, T. et al. (2015) Metabolic gene clusters encoding the enzymes of two branches of the 3-oxoadipate pathway in the pathogenic yeast *Candida albicans*. *FEMS Yeast Research*, 15, fov006.
- Gilchrist, C.L., Booth, T.J., van Wersch, B., van Grieken, L., Medema, M.H. & Chooi, Y.-H. (2021) cblaster: a remote search tool for rapid identification and visualization of homologous gene clusters. *Bioinformatics Advances*, 1, vbab016.
- Gurujeyalakshmi, G. & Mahadevan, A. (1987) Degradation of gallic acid by *Aspergillus flavus*. *Zentralblatt für Mikrobiologie*, 142, 187–192.
- Hartmann, D.O., Shimizu, K., Siopa, F., Leitão, M.C., Afonso, C.A., Lopes, J.N.C. et al. (2015) Plasma membrane permeabilisation by ionic liquids: a matter of charge. *Green Chemistry*, 17, 4587–4598.
- Hatamoto, O., Watarai, T., Kikuchi, M., Mizusawa, K. & Sekine, H. (1996) Cloning and sequencing of the gene encoding tannase and a structural study of the tannase subunit from *Aspergillus oryzae*. *Gene*, 175, 215–221.
- Hawkins, A.R., Lamb, H.K., Moore, J.D., Charles, I.G. & Roberts, C.F. (1993) Review article: the pre-chorismate (shikimate) and quinate pathways in filamentous fungi: theoretical and practical aspects. *Journal of General Microbiology*, 139, 2891–2899.
- Hoff, K.J. & Stanke, M. (2013) WebAUGUSTUS—a web service for training AUGUSTUS and predicting genes in eukaryotes. *Nucleic Acids Research*, 41, W123–W128.
- Holesova, Z., Jakubkova, M., Zavadiaikova, I., Zeman, I., Tomaska, L. & Nosek, J. (2011) Gentisate and 3-oxoadipate pathways in the yeast *Candida parapsilosis*: identification and functional analysis of the genes coding for 3-hydroxybenzoate 6-hydroxylase and 4-hydroxybenzoate 1-hydroxylase. *Microbiology*, 157, 2152–2163.
- Kasai, D., Masai, E., Katayama, Y. & Fukuda, M. (2007) Degradation of 3-O-methylgallate in *Sphingomonas paucimobilis* SYK-6 by pathways involving protocatechuate 4,5-dioxygenase. *FEMS Microbiology Letters*, 274, 323–328.
- Kato, H., Furusawa, T.T., Mori, R., Suzuki, H., Kato, M. & Shimizu, M. (2022) Characterization of two 1,2,4-trihydroxybenzene 1,2-dioxygenases from *Phanerochaete chrysosporium*. *Applied Microbiology and Biotechnology*, 106, 1–11.
- Kim, D., Langmead, B. & Salzberg, S.L. (2015) HISAT: a fast spliced aligner with low memory requirements. *Nature Methods*, 12, 357–360.
- Koseki, T., Ichikawa, K., Sasaki, K. & Shiono, Y. (2018) Characterization of a novel *Aspergillus oryzae* tannase expressed in *Pichia pastoris*. *Journal of Bioscience and Bioengineering*, 126, 553–558.
- Liao, Y., Smyth, G.K. & Shi, W. (2014) featureCounts: an efficient general purpose program for assigning sequence reads to genomic features. *Bioinformatics*, 30, 923–930.
- Love, M.I., Huber, W. & Anders, S. (2014) Moderated estimation of fold change and dispersion for RNA-seq data with DESeq2. *Genome Biology*, 15, 550.
- Lubbers, R.J., Dilokpimol, A., Nousiainen, P.A., Cioc, R.C., Visser, J., Bruijninx, P.C. et al. (2021) Vanillic acid and methoxyhydroquinone production from guaiacyl units and related aromatic compounds using *Aspergillus niger* cell factories. *Microbial Cell Factories*, 20, 1–14.
- Lubbers, R.J.M., Dilokpimol, A., Visser, J., Mäkelä, M.R., Hildén, K.S. & de Vries, R.P. (2019) A comparison between the homocyclic aromatic metabolic pathways from plant-derived compounds by bacteria and fungi. *Biotechnology Advances*, 37, 107396.
- Mäkelä, M.R., Marinović, M., Nousiainen, P., Liwanag, A.J.M., Benoit, I., Sipilä, J. et al. (2015) Chapter two-aromatic metabolism of filamentous fungi in relation to the presence of aromatic compounds in plant biomass. *Advances in Applied Microbiology*, 91, 63–137.
- Martins, T.M., Hartmann, D.O., Planchon, S., Martins, I., Renaut, J. & Silva Pereira, C. (2015) The old 3-oxoadipate pathway revisited: new insights in the catabolism of aromatics in the saprophytic fungus *Aspergillus nidulans*. *Fungal Genetics and Biology*, 74, 32–44.
- Martins, T.M., Martins, C., Guedes, P. & Silva Pereira, C. (2021) Twists and turns in the salicylate catabolism of *Aspergillus terreus*, revealing new roles of the 3-hydroxyanthranilate pathway. *mSystems*, 6, 1, e00230–20.
- Martins, T.M., Martins, C. & Silva Pereira, C. (2019) Chapter five—multiple degrees of separation in the central pathways of the catabolism of aromatic compounds in fungi belonging to the Dikarya sub-Kingdom. In: Poole, R.K. (Ed.) *Advances in microbial physiology*, Vol. 75. USA: Academic Press, pp. 177–203.
- Martins, T.M., Nunez, O., Gallart-Ayala, H., Leitao, M.C., Galceran, M.T. & Silva Pereira, C. (2014) New branches in the degradation pathway of monochlorocatechols by *Aspergillus nidulans*: a metabolomics analysis. *Journal of Hazardous Materials*, 268, 264–272.
- Meier, A.K., Worch, S., Böer, E., Hartmann, A., Mascher, M., Marzec, M. et al. (2017) Agdc1p—a gallic acid decarboxylase involved

- in the degradation of tannic acid in the yeast *Blastobotrys (Arxula) adenivorans*. *Frontiers in Microbiology*, 8, 1777.
- Mingot, J.M., Penalva, M.A. & Fernandez-Canon, J.M. (1999) Disruption of *phacA*, an *Aspergillus nidulans* gene encoding a novel cytochrome P450 monooxygenase catalyzing phenylacetate 2-hydroxylation, results in penicillin overproduction. *The Journal of Biological Chemistry*, 274, 14545–14550.
- Paizs, C., Bartlewski-Hof, U. & Rétey, J. (2007) Investigation of the mechanism of action of pyrogallol–phloroglucinol transhydroxylase by using putative intermediates. *Chemistry—A European Journal*, 13, 2805–2811.
- Patel, T.R., Hameed, N. & Armstrong, S. (1992) Metabolism of gallate in *Penicillium simplicissimum*. *Journal of Basic Microbiology*, 32, 233–240.
- Pathan, M., Keerthikumar, S., Chisanga, D., Alessandro, R., Ang, C.S., Askenase, P. et al. (2017) A novel community driven software for functional enrichment analysis of extracellular vesicles data. *Journal of Extracellular Vesicles*, 6, 1321455.
- Paul, C.E., Eggerichs, D., Westphal, A.H., Tischler, D. & van Berkel, W.J. (2021) Flavoprotein monooxygenases: versatile biocatalysts. *Biotechnology Advances*, 51, 107712.
- Paysan-Lafosse, T., Blum, M., Chuguransky, S., Grego, T., Pinto, B.L., Salazar, G.A. et al. (2023) InterPro in 2022. *Nucleic Acids Research*, 51, D418–D427.
- Ramírez-Coronel, M.A., Viniestra-Gonzalez, G., Darvill, A. & Augur, C. (2003) A novel tannase from *Aspergillus niger* with β -glucosidase activity. *Microbiology*, 149, 2941–2946.
- Semana, P. & Powlowski, J. (2019) Four aromatic Intradiol ring cleavage dioxygenases from *Aspergillus niger*. *Applied and Environmental Microbiology*, 85, e01786–01719.
- Sietmann, R., Uebe, R., Böer, E., Bode, R., Kunze, G. & Schauer, F. (2010) Novel metabolic routes during the oxidation of hydroxylated aromatic acids by the yeast *Arxula adenivorans*. *Journal of Applied Microbiology*, 108, 789–799.
- Szewczyk, E., Nayak, T., Oakley, C.E., Edgerton, H., Xiong, Y., Taheri-Talesh, N. et al. (2007) Fusion PCR and gene targeting in *Aspergillus nidulans*. *Nature Protocols*, 1, 3111–3120.
- Watanabe, A. (1965) Studies on the metabolism of gallic acid by microorganisms: part III. On the intermediary metabolism of gallic acid by *Aspergillus niger*. *Agricultural and Biological Chemistry*, 29, 20–26.
- Weiss, A.K., Loeffler, J.R., Liedl, K.R., Gstach, H. & Jansen-Dürr, P. (2018) The fumarylacetoacetate hydrolase (FAH) superfamily of enzymes: multifunctional enzymes from microbes to mitochondria. *Biochemical Society Transactions*, 46, 295–309.
- Ye, J., Coulouris, G., Zaretskaya, I., Cutcutache, I., Rozen, S. & Madden, T.L. (2012) Primer-BLAST: a tool to design target-specific primers for polymerase chain reaction. *BMC Bioinformatics*, 13, 1.
- Zhao, X., Zhi, Q.-Q., Li, J.-Y., Keller, N.P. & He, Z.-M. (2018) The antioxidant gallic acid inhibits aflatoxin formation in *Aspergillus flavus* by modulating transcription factors FarB and CreA. *Toxins*, 10, 270.

SUPPORTING INFORMATION

Additional supporting information can be found online in the Supporting Information section at the end of this article.

How to cite this article: Martins, T.M., Bento, A., Martins, C., Tomé, A.S., Moreira, C.J.S. & Silva Pereira, C. (2024) Bringing up to date the toolkit for the catabolism of aromatic compounds in fungi: The unexpected 1,2,3,5-tetrahydroxybenzene central pathway. *Microbial Biotechnology*, 17, e14371. Available from: <https://doi.org/10.1111/1751-7915.14371>